Provided for non-commercial research and education use.
Not for reproduction, distribution or commercial use.

This article appeared in a journal published by Elsevier. The attached copy is furnished to the author for internal non-commercial research and education use, including for instruction at the authors institution and sharing with colleagues.

Other uses, including reproduction and distribution, or selling or licensing copies, or posting to personal, institutional or third party websites are prohibited.

In most cases authors are permitted to post their version of the article (e.g. in Word or Tex form) to their personal website or institutional repository. Authors requiring further information regarding Elsevier's archiving and manuscript policies are encouraged to visit:

http://www.elsevier.com/copyright

Author's personal copy

Journal of Food Engineering 105 (2011) 485–492

Contents lists available at ScienceDirect

Journal of Food Engineering

journal homepage: www.elsevier.com/locate/jfoodeng

Automated fish bone detection using X-ray imaging

Domingo Mery *, Iván Lillo, Hans Loebel, Vladimir Riffo, Alvaro Soto, Aldo Cipriano, José Miguel Aguilera

Pontificia Universidad Católica de Chile, Chile

ARTICLE INFO

Article history:
Received 15 October 2010
Received in revised form 2 March 2011
Accepted 6 March 2011
Available online 16 March 2011

Keywords:
Fish bones
X-ray testing
Computer vision
Automated visual inspection
Salmon
Trout

ABSTRACT

In countries where fish is often consumed, fish bones are some of the most frequently ingested foreign bodies encountered in foods. In the production of fish fillets, fish bone detection is performed by human inspection using their sense of touch and vision which can lead to misclassification. Effective detection of fish bones in the quality control process would help avoid this problem. For this reason, an X-ray machine vision approach to automatically detect fish bones in fish fillets was developed. This paper describes our approach and the corresponding experiments with salmon and trout fillets. In the experiments, salmon X-ray images using 10×10 pixels detection windows and 24 intensity features (selected from 279 features) were analyzed. The methodology was validated using representative fish bones and trouts provided by a salmon industry and yielded a detection performance of 99%. We believe that the proposed approach opens new possibilities in the field of automated visual inspection of salmon, trout and other similar fish.

© 2011 Elsevier Ltd. All rights reserved.

1. Introduction

Since Röntgen discovered in 1895 that X-rays can identify inner structures, the technology has been developed not only for use in *medical imaging* for human beings, but also for *non-destructive testing* (NDT) of materials and objects (Richter, 1999), where the aim is to analyze internal elements that are undetectable to the naked eye. NDT with X-rays, called *X-ray testing*, is used in many applications such as: food product analysis (Haff and Toyofuku, 2008), baggage screening (Zentai, 2008), automotive parts inspection (Mery, 2006), and welding quality control (Silva and Mery, 2007), among others.

X-ray testing can be performed by human inspection or automated systems. Although humans perform better than machines in many cases, they are slower and can get tired quickly. Another disadvantage to human inspection stems from every product needing to be 100% checked to ensure consumer safety, these inspections typically require a high level of redundancy which in turn increases cost and inspection time (Newman and Jain, 1995; Hardmeier et al., 2005; Brandt, 2000). Automated systems are objective and can be reproduced identically for every test giving it an impressive advantage over manual X-ray testing. In general human inspection is at best 80% effective (Newman and Jain, 1995). In order to achieve efficient and effective X-ray testing, automated systems are being developed to execute this difficult, tedious and sometimes dangerous task.

In food safety, several applications using X-ray testing have been developed for the industry (Davies, 2000). The inherent difficulties in detecting defects, foreign objects and contaminants in food products have limited the use of X-ray to the packaged foods sector (Kwon et al., 2008). However, the necessity for NDT has motivated a considerable research effort in this field spanning many decades (Haff and Toyofuku, 2008). Important advances include: bone detection in poultry production (Graves, 2003), identification of insect infestation in citrus (Jiang et al., 2008), detection of codling moth larvae in apples (Haff and Toyofuku, 2008), fruit quality inspection like split-pits, water content distribution and internal structure (Ogawa et al., 2003), and detection of the granary weevil's larval stages in wheat kernels (Haff and Slaughter, 2004).

In the automated detection of fish bones, often called pin bones, there are few published papers: Andersen (2003) mentioned the basic components of a processing line to remove fish bones using a *pin bone detection unit*, however, there is no documentation for how the detection works. Han and Shi (2007) developed an approach with 85% effectiveness in fish bone detection based on *particle swarm clustering* in regions of interest obtained by thresholding and morphological operations. Lorencs et al. (2009) elaborated on a general algorithm based on statistical features that can be used to detect fish bones, in which small vertical fragments are segmented in gray value images containing a varying undefined background, however, validation experiments are not reported. Thielemann et al. (2007) presented an interesting method based on texture analysis of the surface image (not an X-ray image) to predict the positions where fish bones could be present in the

* Corresponding author.
E-mail address: dmery@ing.puc.cl (D. Mery).
URL: http://dmery.ing.puc.cl (D. Mery).

0260-8774/$ - see front matter © 2011 Elsevier Ltd. All rights reserved.
doi:10.1016/j.jfoodeng.2011.03.007

Author's personal copy

Fig. 1. Typical human inspection in a processing line using pliers to remove fish bones in salmon fillets.

fillet. In the literature review, we observed the lack of an approach that could automatically detect fish bones effectively. That is most likely due to the fact that X-ray images of fish fillets with fish bones are very similar to those images where the texture of the surrounding fish fillet is present (Andersen, 2003). For this reason, in this work the aim was to solve this problem using modern computer vision techniques. To the best of our knowledge, this is the first time that these techniques are used in automated fish bone detection. X-ray testing is playing an increasingly important role in food quality assurance. However, fish bone detection in fish fillets is mainly performed by human inspection using touch and vision senses which can certainly lead to misclassification, as shown in Fig. 1. In countries where fish is often consumed, fish bones are one of the most frequently ingested foreign bodies encountered in foods (Akazawa et al., 2004), so effective fish bone detection in quality control would assist in avoiding this problem. For this reason, we developed an X-ray machine vision approach to detect fish bones in fish fillets automatically with high performance. This paper describes the proposed approach and the corresponding validation experiments with salmon and trout fillets. A previous version of this paper can be found in (Mery et al., 2010) where preliminary results on salmons were presented.

The rest of the paper is organized as follows: In Section 2, the proposed X-ray machine vision approach is explained. In Section 3, the results obtained in several experiments on salmon and trout fillets are shown. Finally, in Section 4 some concluding remarks are given.

2. Detection of fish bones

The key idea of this work is to use a machine vision methodology, as shown in Fig. 2, to automatically detect fish bones in fish fillets. The steps involved in this methodology are (Gonzalez and Woods, 2008): image acquisition, pre-processing, segmentation, feature extraction, classification and post-processing.

2.1. Image acquisition

The X-ray source generates X-ray photons which irradiate the inspected fish fillet. The fish fillet absorbs energy according to the principle of *differential absorption* (Haken and Wolf, 2000). Thus, internal elements of the fillet (such as fish bones, regular structures of the muscles, discontinuities, or foreign objects) modify the expected radiation received by the X-ray detector (Halmshaw, 1991). In these experiments, as shown in Fig. 3, we used:

- *X-ray source:* A battery powered X-ray system Poskom XM-20BT (tube focal spot: 1.2 mm, max. output: 100 kV, 20 mA).
- *Flat panel detector:* A digital radiography system Cannon CXDI-50G (detection size: 35×43 cm^2, image size: 2.208×2.688 pixels (5.93 million pixels), pixel size: 160 μm, gray-scale: 4.096 (12-bits) gray value).

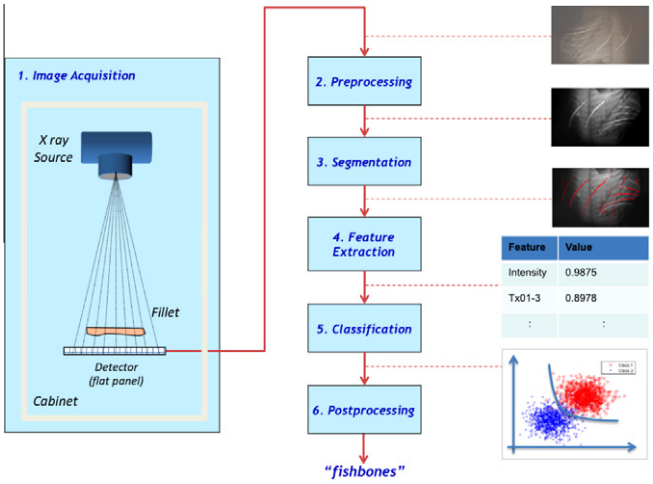

Fig. 2. Machine vision schema used to automatically detect fish bones in fish fillets.

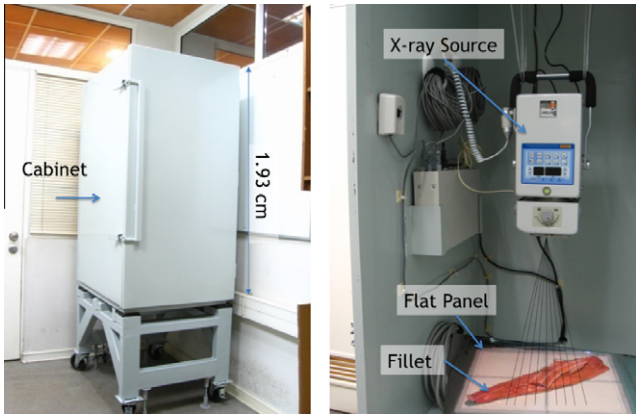

Fig. 3. X-ray imaging system: X-ray source, flat panel and fillet are enclosed in a lead cabinet that provides enough radiation attenuation.

The X-ray source, the fish fillet exposed to X-rays, and the flat panel detector are enclosed in a lead cabinet that provides enough radiation attenuation and prevents access to the X-ray beam. The voltage and composite factor of the X-ray source were set to 40 kV and 21 mA, respectively, by maximizing the contrast and minimizing the noise of more than twenty X-ray images of salmon fillets (Fig. 4).

2.2. Pre-processing and segmentation

The fish bones are only present in certain space frequencies of the spectrum: they are not too thin (minimal 0.5 mm) nor too thick

Author's personal copy

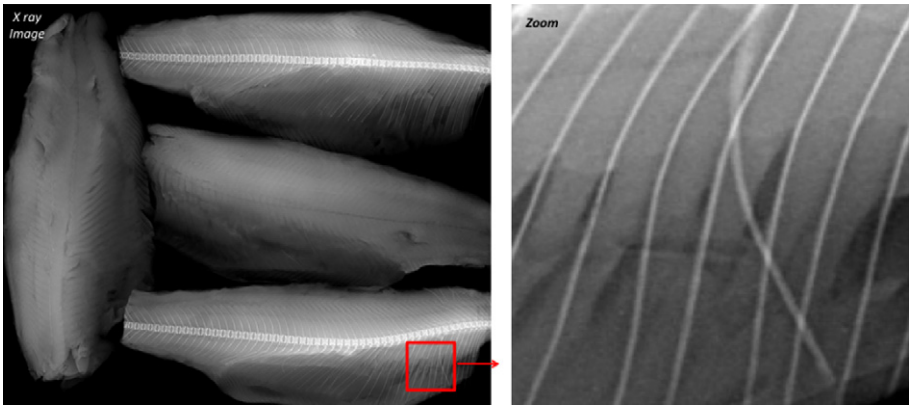

Fig. 4. X-ray image of fish fillets in which the fish bones are detectable.

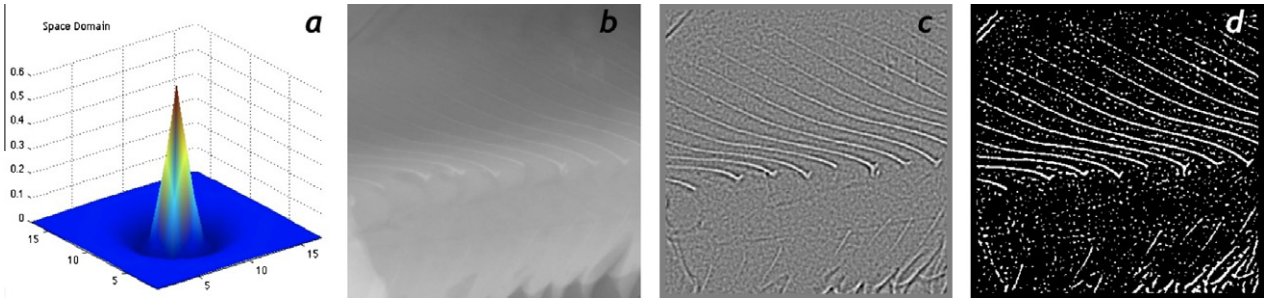

Fig. 5. Segmentation of potential fish bones: (a) convolution mask **H** in space domain, (b) original X-ray image **X** of a salmon fillet, (c) filtered image **Z**, (d) potential fish bones image **P** after thresholding and removing objects deemed too small.

(maximal 2 mm). The segmentation of potential fish bones is based on a band pass filter to enhance the fish bones with respect to their surroundings as shown in Fig. 5. The proposed approach to detect potential fish bones has four steps:

- *Enhancement:* The original X-ray image **X** (Fig. 5b) is enhanced linearly by modifying the original histogram in order to increase contrast (Gonzalez and Woods, 2008): The enhanced image **Y** is:

$$\mathbf{Y} = a\mathbf{X} + b \tag{1}$$

- *Band pass filtering:* The enhanced image **Y** is filtered using a radial symmetric 17×17 pixels mask **H** (Fig. 5a). Mask **H** was estimated from 20 X-ray images by minimizing the error rate as mention by Canny (1986) and applied to fish bones (all fish bones should be found and there should be no false alarms). The filtered image **Z** (Fig. 5c) is then the convolution of **Y** with mask **H**:

$$\mathbf{Z} = \mathbf{Y} * \mathbf{H} \tag{2}$$

- *Thresholding:* Those pixels in **Z** that have gray values greater than a certain threshold θ are marked in a binary image **B**. The threshold is defined to ensure that all fish bones are detected, i.e., false alarms are allowed in this step. The pixels of **B** are defined as:

$$B_{ij} = \begin{cases} 1 & \text{if } Z_{ij} > \theta \\ 0 & \text{else} \end{cases} \tag{3}$$

- *Removal of small objects:* All connected pixels in **B** containing fewer than A pixels are removed as shown in Fig. 5d. This image, called **P**, defines the potential fish bones.

2.3. Feature extraction and selection

The segmented potential fish bones – contained in image **P** – are divided into small 10×10 pixels windows called *detection windows*. In a training phase, using a priori knowledge of the fish bones, the detection windows are manually labeled as one of two classes: *bones* and *no-bones*. The first class corresponds to those regions where the potential fish bones are indeed fish bones. Alternatively, the second class corresponds to false alarms. Intensity features of the enhanced X-ray image **Y** are extracted for both classes. We use enhanced image **Y**, instead of pre-processed image **X**, because after our experiments the detection performance was higher. Features extracted from each area of an X-ray image region are divided into four groups as shown in Table 1:

- *Standard:* Simple intensity information related to the mean intensity in the region; standard deviation of the intensity in the region, and in the image; mean first derivative in the boundary of the region; and second derivative in the region (Nixon and Aguado, 2008). There are five standard features.
- *Statistical textures:* Texture information extracted from the distribution of the intensity values based on the Haralick (1979) approach. They are computed utilizing *co-occurrence matrices* that represent second order texture information (the joint probability distribution of intensity pairs of neighboring pixels in the image), where mean and range – for five different pixel distances – of the following variables were measured: (1) Angular Second Moment, (2) Contrast, (3) Correlation, (4) Sum of Squares, (5) Inverse Difference Moment, (6) Sum Average, (7) Sum Entropy, (8) Sum Variance, (9) Entropy, (10) Difference Variance, (11) Difference Entropy, (12 and

Author's personal copy

Table 1
Extracted features.

Group	Number	Name and references
1. Standard	5	Mean intensity in the region; standard deviation of the intensity in the region, and in the image; mean first derivative in the boundary of the region; and second derivative in the region (Nixon and Aguado, 2008)
2. Statistical textures	140	Tx(k,p) (mean/range) for k = (1) Angular Second Moment, (2) Contrast, (3) Correlation, (4) Sum of Squares, (5) Inverse Difference Moment, (6) Sum Average, (7) Sum Entropy, (8) Sum Variance, (9) Entropy, (10) Difference Variance, (11) Difference Entropy, (12 and 13) Information Measures of Correlation, (14) Maximal Correlation Coefficient, and p=1, . . . ,5 pixels (Haralick, 1979)
3. Filter banks	75	DFT (1,2;1,2) and DCT (1,2;1,2) (Gonzalez and Woods, 2008). Gabor (1,. . .,8;1,. . .,8), max(Gabor), min(Gabor), Gabor-J = max–min (Kumar and Pang, 2002)
4. Local binary patterns	59	LBP (1, . . . ,59) (Ojala et al., 2002)

13) Information Measures of Correlation, and (14) Maximal Correlation Coefficient. There are $2 \times 14 \times 5 = 140$ statistical features.

- *Filter banks:* Texture information extracted from image transformations like Discrete Fourier Transform (DFT), Discrete Cosine Transform (DCT) (Gonzalez and Woods, 2008), and Gabor features based on 2D Gabor functions, i.e., Gaussian-shaped band-pass filters, with dyadic treatment of the radial spatial frequency range and multiple orientations, which represent an appropriate choice for tasks requiring simultaneous measurement in both space and frequency domains (usually 8 scale and 8 orientations). Additionally, the maximum, the minimum and the difference between both are computed (Kumar and Pang, 2002). There are 4 DCT features, 4 Fourier features and $8 \times 8 + 3$ Gabor features, i.e., 4 + 4 + 67 = 75 Filter bank features.
- *Local binary patterns:* Texture information extracted from occurrence histogram of *local binary patterns* (LBP) computed from the relationship between each pixel intensity value with its eight neighbors. The features are the frequencies of each one of the histogram's 59 bins. LBP is very robust in terms of gray-scale and rotation variations (Ojala et al., 2002). There are 59 LBP features.

In these experiments, $n = 5 + 140 + 75 + 59 = 279$ features are extracted from each detection window. Afterwards, the features must be selected in order to decide on the relevant features for the two defined classes.

The n extracted features for sample i are arranged in an n-vector: $\mathbf{f}_i = [f_{i1} \cdots f_{in}]$ that corresponds to a point in the n-dimensional measurement feature space. The features are normalized yielding a $N \times n$ matrix $\mathbf{W}$ which elements are defined as:

$$w_{ij} = \frac{f_{ij} - \mu_j}{\sigma_j} \tag{4}$$

for $i = 1, \ldots, N$ and $j = 1, \ldots, n$, where f_{ij} denotes the jth feature of the ith feature vector, N is the number of samples and μ_j and σ_j are the mean and standard deviation of the jth feature. Thus, the normalized features have zero mean and a standard deviation equal to one. Those high correlated features can be eliminated because they do not provide relevant information about the food evaluation quality.

In feature selection, a subset of m features ($m < n$) that leads to the smallest classification error is selected. The selected m features are arranged in a new m-vector $\mathbf{s}_i = [s_{i1} \cdots s_{im}]$. This can be understood as a matrix $\mathbf{S}$ with $N \times m$ elements obtained from m selected columns of the large set of normalized features $\boldsymbol{W}$.

The features can be selected using several state-of-art algorithms documented in literature like Forward Orthogonal Search (Wei and Billings, 2007), Least Square Estimation (Mao, 2005), Ranking by Class Separability Criteria (MathWorks, 2007) and Combination with Principal Components (Bishop, 2006) among others. However, in the experiments the best performance was achieved using the well-known Sequential Forward Selection

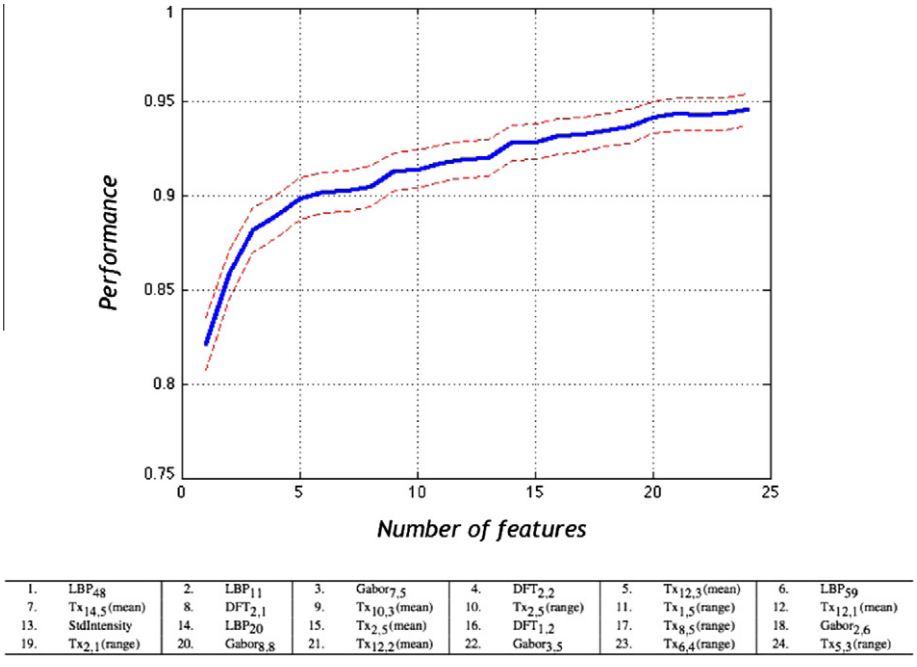

Fig. 6. Classification performance with a 95% confidence interval using the first m features (refer to Table 1 to see a description of the features).

Author's personal copy

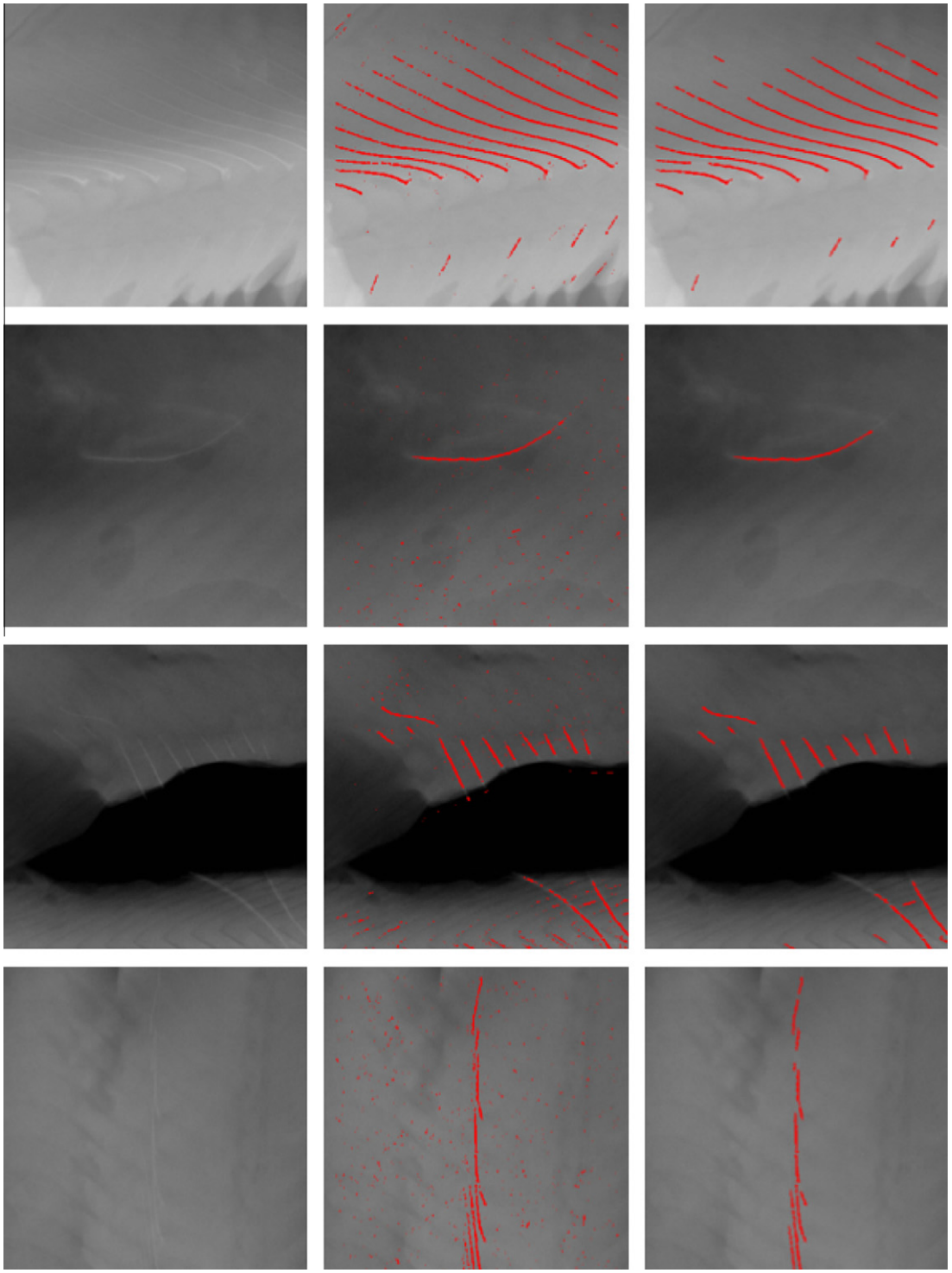

Fig. 7. Results obtained in four X-ray images. The columns correspond to enhanced images, classified fish bones and post-processed fish bones. The first row corresponds to the example shown in Fig. 5.

(SFS) algorithm (Jain et al., 2000). This method selects the best single feature and then adds one feature at a time that, in combination with the selected features, maximizes classification performance. The iteration is halted once no considerable improvement in the performance is achieved by adding a new feature. By evaluating selection performance we ensure: (i) a small intraclass variation and (ii) a large interclass variation in the space of the selected features. For the first and second conditions the intraclass-covariance $\mathbf{C}_b$ and interclass-covariance $\mathbf{C}_w$ of the selected features $\mathbf{S}$ are used, respectively (Bishop, 2006). Selection performance can be evaluated using:

$$J(\mathbf{S}) = \mathrm{trace}\left(\mathbf{C}_w^{-1}\mathbf{C}_b\right), \tag{5}$$

where 'trace' means the sum of the diagonal elements. The larger the objective function J, the higher the selection performance.

Author's personal copy

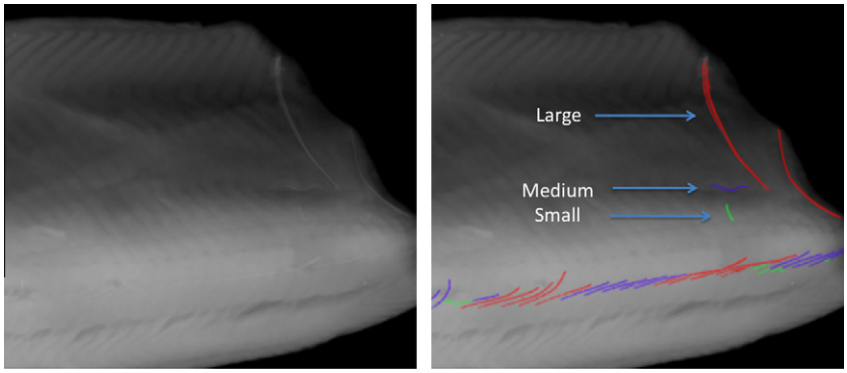

Fishbone	Sensibility	1-Specificity	Size
Large	100%	0%	>0.64mmx12mm
Medium	100%	3%	between
Small	93%	6%	<0.48mmx8.5mm

Fig. 8. Results obtained on 3878 samples using cross-validation with 5 folds.

2.4. Classification and validation

A classifier decides whether the detection windows are *bones* or *no-bones*. We tested several classifiers, such as statistical or those based on neural networks (Bishop, 2006), however, the best performance was achieved using Support Vector Machines (SVM) (Shawe-Taylor and Cristianini, 2004). SVM transforms a two-class feature space, where the classes overlap, into a new enlarged feature space where the classification boundary is linear. Thus, a simple linear classification can be designed in the transformed feature space in order to separate both classes . The original feature space is transformed using a function $h(\mathbf{s})$, however, for the classification only the kernel function $K(\mathbf{s},\mathbf{s}') = \langle h(\mathbf{s}), h(\mathbf{s}')\rangle$ that computes inner products in the transformed space is required. In the experiments, the best classification was obtained using a *Gaussian Radial Basis* (RBF) function kernel defined by (Hastie et al., 2003):

$$K(\mathbf{s},\mathbf{s}') = e^{-||\mathbf{s}-\mathbf{s}'||^2} \tag{6}$$

where the linear boundary, i.e., the separating hyperplane in the transformed space, is computed using the Least Squares approach (MathWorks, 2007).

The performance of the classifier was defined as the ratio of the detection windows that were correctly classified to the total number of detection windows. The performance was validated using cross-validation, a technique widely implemented in machine learning problems (Mitchell, 1997). In cross-validation, the samples are divided into F folds randomly. $F-1$ folds are used as training data and the remaining fold is used as testing data to evaluate the performance of the classifiers. This experiment is repeated F times rotating train and test data. The F individual performances from the folds are averaged to estimate the final performance of the classifiers.

3. Experimental results

First, the proposed method was tested with 20 representative salmon fillets obtained at a local fish market. The average size of these fillets was 15×10 cm^2. According to pre-processing and segmentation techniques explained in Section 2.2, several regions of interest were obtained where fish bones could be located. The area occupied by these regions of interest corresponds to approx. 12% of the salmon fillets as shown in Fig. 5.

From the mentioned regions of interest 7697 detection windows of 10×10 pixels were obtained. Each window was labeled with '1' for class *bones* and '0' for *no-bones*. From each window, 279 features were extracted according to Section 2.3. After the feature extraction, 75% of the samples from each class were randomly chosen to perform the feature selection. The best performance was achieved using Sequential Forward Selection. The best 24 features are shown in Fig. 6 in ascending order. The features give information about the spatial distribution of pixels, i.e., how coarse or fine the texture is. According to Table 1, the selected features correspond mainly to statistical features (12) and filter banks (7), however, it is worth to note the most two discriminative features are LBP features (in this case LBP 48 and LBP 11). On the other hand, from the standard features there is only one feature (standard deviation of the intensity).

The best performance was achieved by a SVM classifier. Using cross-validation with $F = 10$ folds, the proposed method was validated for m selected features, for $m = 1,\ldots,24$, as shown in Fig. 6. The 95% confidence interval was always ±1% approximately. The higher the number of selected features the higher the performance, however, for more than 24 features, no more significant increase in the performance was obtained. The results show that by using 24 features, the performance was almost 94.7% with a 95% confidence interval between 94.3% and 95.1%. Fig. 7 shows the final detection in four cases.

In order to investigate the sensibility (S_n) and 1-specificity ($1-S_p$) of the fish bones depending on the largeness, three size groups were built: *large* for fish bones larger than 12 mm, *small* for fish bones smaller than 8.5 mm, and *medium* for fish bones between both sizes. In this experiment, 3878 fish bones were manually selected. The performance was calculated using a cross-validation with 5 folds. The results are summarized in Fig. 8. All medium and large fish bones were detected (with $1-S_p = 0\%$ and 3%, respectively), whereas 93% of small fish bones were correctly detected with $1-S_p = 6\%$. This means that cross-validation yielded a detection performance of 100%, 98.5% and 93.5% (computed using $(S_n + S_p)/2$) for large, medium and small fish bones, respectively.

Finally, in order to validate the proposed methodology, the last experiment was carried out using representative fish bones and representative trout fillets provided by a Chilean salmon industry.

Author's personal copy

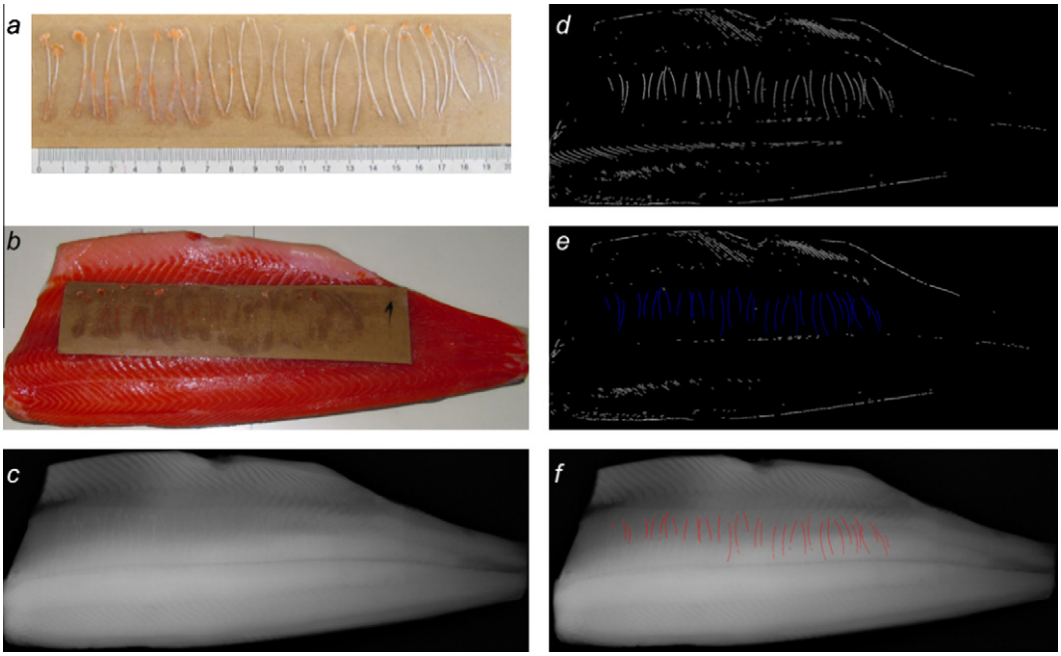

Fig. 9. Results obtained on a trout fillet using a fish bone strip with 33 fish bones: (a) strip, (b) strip over the fillet, (c) X-ray image, (d) segmentation, (e) classification, (f) post-processing. All fish bones were detected ($S_n = 1$), in this example there was no false alarm ($1 - S_p = 0$).

The size of the fish bones were between 14 and 47 mm (larger than the small-size and mid-size groups considered above). The fish bones were arranged in strips that were superimposed onto trout fillets. Thus, the number of fish bones to be detected was a priori known. According to the absorption law, an X-ray image of a fillet with a fish bone inside, and an X-ray image with a fish bone laid on the fillet top are almost identical. Similar methodologies are used in industrial X-ray inspection of materials in order to simulate discontinuities (Mery, 2001). The only difference could be that the position of a real fish bone (inside of a fillet) achieves a more realistic location related to the fish tissues, however, after our experience, the obtained images are very similar. Fig. 9 shows the detection of one fish bone strip on a trout fillet. Using the same classifier trained in the last experiment, i.e., no new training was necessary, the proposed method was able to detect all fish bones with a 1% false positive rate. In this case, 15 X-ray images were tested, with 459 *bones* and 10,413 *no-bones*.

The developed computational program was implemented in Visual C on a PC, equipped with two Intel Xeon CPUs, at 2.5 GHz, with 4 Gb RAM, running under Windows XP. The computational time was about 0.3 s for each fillet of 150 cm^2. Each X-ray image captured 3 of such fillets, because the flat panel covers 500 cm^2. The processing time is good enough for a real time implementation, however, the used acquisition system requires 12 s to transmit each X-ray digital image from flat panel to PC. This means, the proposed computer vision system can be used in real time only if a faster acquisition X-ray system is used, e.g., a digital X-ray system live.

4. Conclusion

The need for more information on the quality control of several fish types by means of quantitative methods can be satisfied using X-ray testing, a non-destructive technique that can be used to measure, objectively, intensity and geometric patterns in non-uniform surfaces. In addition the method can also determine other physical features such as image texture, morphological elements, and defects in order to automatically determine the quality of a fish fillet. The promising results outlined in this work show that a very high classification rate was achieved in the quality control of salmon and trout when using a large number of features combined with efficient feature selection and classification. The key idea of the proposed method was to select, from a large universe of features, only those features that were relevant for the separation of the classes. Cross validation yielded a detection performance of 100%, 98.5% and 93.5% for large, medium and small fish bones, respectively. The proposed method was validated on trouts with representative fish bones provided by a Chilean salmon industry yielding a performance of 99%. Although the method was validated with salmon and trout fillets only, we believe that the proposed approach opens new possibilities not only in the field of automated visual inspection of salmons and trouts but also in other similar fish.

Acknowledgment

The authors would like to thank to Grant Fondef–Chile No. D07I1080 – Chile and Ventisqueros S.A.–Chile.

References

Akazawa, Y., Watanabe, S., Nobukiyo, S., Iwatake, H., Seki, Y., Umehara, T., Tsutsumi, K., Koizuka, I., 2004. The management of possible fishbone ingestion. Auris Nasus Larynx 31 (4), 413–416.

Andersen, K., 2003. X-ray techniques for quality assessment. In: Luten, J.B., Oehlenschläeger, J., Olafsdottir, G. (Eds.), Quality of Fish from Catch to Consumers. Wageningen Academic Publishers, pp. 283–286.

Bishop, C.M., 2006. Pattern Recognition and Machine Learning. Springer.

Brandt, F., 2000. The use of X-ray inspection techniques to improve quality and reduce costs. The e-Journal of Nondestructive Testing & Ultrasonics 5 (5) (www.ndt.net).

Canny, J., 1986. A computational approach to edge detection. IEEE Transactions on Pattern Analysis and Machine Intelligence (PAMI) 8 (6), 679–698.

Davies, E., 2000. Image Processing for the Food Industry. World Scientific.

Gonzalez, R., Woods, R., 2008. Digital Image Processing, third ed. Pearson, Prentice Hall.

Graves, M., 2003. X-ray bone detection in further processed poultry production. Machine Vision for the Inspection of Natural Products, 421–449.

Haff, R., Slaughter, D., 2004. Real-time X-ray inspection of wheat for infestation by the granary weevil, sitophilus granarius (l.). Transactions of the American Society of Agricultural Engineers 47, 531–537.

Haff, R., Toyofuku, N., 2008. X-ray detection of defects and contaminants in the food industry. Sensing and Instrumentation for Food Quality and Safety 2 (4), 262–273.

Author's personal copy

Haken, H., Wolf, H., 2000. The Physics of Atoms and Quanta: Introduction to Experiments and Theory, sixth ed. Springer, Berlin, Heidelberg.
Halmshaw, R., 1991. Non-Destructive-Testing, second ed. Edward Arnold, London.
Han, Y., Shi, P., 2007. An efficient approach for fish bone detection based on image preprocessing and particle swarm clustering. Communications in Computer and Information Science 21, 940–948.
Haralick, R., 1979. Statistical and structural approaches to texture. Proceedings of the IEEE 67 (5), 786–804.
Hardmeier, D., Hofer, F., Schwaninger, A., 2005. The X-ray object recognition test (X-ray ort) – a reliable and valid instrument for measuring visual abilities needed in X-ray screening. In: 39th Annual 2005 International Carnahan Conference on Security Technology (CCST'05), pp. 189–192.
Hastie, T., Tibshirani, R., Friedman, J., 2003. The Elements of Statistical Learning: Data Mining, Inference, and Prediction, corrected ed. Springer.
Jain, A., Duin, R., Mao, J., 2000. Statistical pattern recognition: a review. IEEE Transactions on Pattern Analysis and Machine Intelligence 22 (1), 4–37.
Jiang, J., Chang, H., Wu, K., Ouyang, C., Yang, M., Yang, E., Chen, T., Lin, T., 2008. An adaptive image segmentation algorithm for X-ray quarantine inspection of selected fruits. Computers and Electronics in Agriculture 60, 190–200.
Kumar, A., Pang, G., 2002. Defect detection in textured materials using Gabor filters. IEEE Transactions on Industry Applications 38 (2), 425–440.
Kwon, J., Lee, J., Kim, W., 2008. Real-time detection of foreign objects using X-ray imaging for dry food manufacturing line. In: Proceedings of IEEE International Symposium on Consumer Electronics (ISCE2008), pp. 1–4.
Lorencs, A., Medniek, I., Sinica-Sinavskis, J., 2009. Fast object detection in digital grayscale images. Proceedings of the Latvian Academy of Sciences, Section B: Natural, Exact, and Applied Sciences 63 (3), 116–124.
Mao, K., 2005. Identifying critical variables of principal components for unsupervised feature selection. IEEE Transactions on Systems, Man, and Cybernetics, Part B: Cybernetics 35 (2), 339–344.
MathWorks, 2007. Matlab Toolbox of Bioinformatics: User's Guide. Mathworks Inc.
Mery, D., 2001. Flaw simulation in castings inspection by radioscopy. Insight 43 (10), 664–668.
Mery, D., 2006. Automated radioscopic testing of aluminum die castings. Materials Evaluation 64 (2), 135–143.
Mery, D., Lillo, I., Loebel, H., Riffo, V., Soto, A., Cipriano, A., Aguilera, J., 2010. Automated detection of fish bones in salmon fillets using X-ray testing. In: Fourth Pacific-Rim Symposium on Image and Video Technology (PSIVT2010), Singapore, November 14–17, 2010, pp. 1–6.
Mitchell, T., 1997. Machine Learning. McGraw-Hill, Boston.
Newman, T., Jain, A., 1995. A survey of automated visual inspection. Computer Vision and Image Understanding 61 (2), 231–262.
Nixon, M., Aguado, A., 2008. Feature Extraction and Image Processing, second ed. Academic Press.
Ogawa, Y., Kondo, N., Shibusawa, S., 2003. Inside quality evaluation of fruit by X-ray image. In: International IEEE/ASME Conference on Advanced Intelligent Mechatronics (AIM2003), vol. 2, pp. 1360–1365.
Ojala, T., Pietikainen, M., Maenpaa, T., 2002. Multiresolution gray-scale and rotation invariant texture classification with local binary patterns. IEEE Transactions on Pattern Analysis and Machine Intelligence 24 (7), 971–987.
Richter, H.-U., 1999. Chronik der Zerstörungsfreien Materialprüfung, first ed. Deutsche Gesellschaft für Zerstörungsfreie Prüfung, DGZfP, Verlag für Schweißen und verwendete Verfahren, DVS-Verlag GmbH, Berlin.
Shawe-Taylor, J., Cristianini, N., 2004. Kernel Methods for Pattern Analysis. Cambridge University Press.
Silva, R., Mery, D., 2007. State-of-the-art of weld seam inspection using X-ray testing: Part I. Image processing. Materials Evaluation 65 (6), 643–647.
Thielemann, J., Kirkhus, T., Kavli, T., Schumann-Olsen, Haugland, O., Westavik, H., 2007. System for estimation of pin bone positions in pre-rigor salmon. In: Lecture Notes in Computer Science. Advanced Concepts for Intelligent Vision Systems (ACIVS2007), vol. 4678, pp. 888–896.
Wei, H.-L., Billings, S., 2007. Feature subset selection and ranking for data dimensionality reduction. IEEE Transactions on Pattern Analysis and Machine Intelligence 29 (1), 162–166.
Zentai, G., 2008. X-ray imaging for homeland security. In: IEEE International Workshop on Imaging Systems and Techniques (IST2008), pp. 1–6.